A New M-ary/SSMA Scheme Applicable in LEO Satellite Communication Systems

Tadahiro WADA, Takaya YAMAZATO, Masaaki KATAYAMA, and Akira OGAWA
Department of Information Electronics, Nagoya University
Furo-cho, Chikusa-ku, Nagoya, 464-01 JAPAN.
Tel.:+81-52-789-2729 Fax:+81-52-789-3173 E-mail:wada@ogawa.nuee.nagoya-u.ac.jp

Abstract—**In this paper, we discuss a non-coherent reception of M-ary spread-spectrum multiple-access (M-ary/SSMA) signals in the presence of large Doppler frequency shift.**

The Hadamard Codes (H-codes) is applied as orthogonal codes. The influence of Doppler frequency shift has a particular characteristic according to the property of H-codes. Making use of this property, we, first, propose an initial carrier frequency acquisition method which can estimate the value of large Doppler frequency shift. We, then, proposed a M-ary/SSMA scheme that is based on the simultaneous transmission of two distinctive H-codes.

I. Introduction

Recently, there have been many studies on the application of spread-spectrum multiple-access(SSMA) scheme for Low Earth-Orbit (LEO) satellite communication systems. It is said that the use of SSMA schemes in LEO satellite communication systems offers higher spectrum efficiency than non-spread schemes. In addition, the SSMA schemes are effective in mitigating multipath fading because of their wide bandwidth [1][2].

M-ary spread-spectrum multiple-access (M-ary/SSMA) scheme has been also drawing much attention in the area of spread-spectrum communications [3]-[9]. M-ary/SSMA scheme is based on the modulation with a set of orthogonal codes. With this scheme, by increasing the grade of multiplicity, one can expect higher spectral efficiency than the conventional direct-sequence spread-spectrum (DS/SS) scheme, in which the signal spectra are spread on bit-by-bit basis with PN sequences. Unlike the phase-coded DS/SS signals, here it is possible to demodulate M-ary/SS signals non-coherently with sufficient quality. For these reasons, it can be expected that M-ary/SSMA schemes can be useful for LEO satellite communication systems.

In LEO satellite communications, large Doppler frequency shift is caused by the difference of velocities between the earth and LEO satellites. The value of Doppler frequency shift may be often larger than ten times of symbol rate. In the presence of large Doppler frequency shift, a considerable degradation in the non-coherent reception of spread-spectrum signals is predicted [6]-[9].

In this paper, we discuss a non-coherent reception of M-ary/SSMA signals in the presence of large Doppler frequency shift. The orthogonal codes generated by the Hadamard Matrix (H-codes) is considered. We deal with the large Doppler frequency shift such as 5 times of symbol rate.

This work is partly supported by NTT Mobile Communication Network Inc. (NTT DoCoMo) and the Ministry of Education, Science, Sports and Culture of Japan under Grant-in-Aid for Scientific Research-A No.08750426.

In order to overcome the effect of the Doppler frequency shift, we, first, show that the influences of Doppler frequency offset have the particular characteristic according to the property of H-codes. Making use of this property, we propose an initial carrier frequency acquisition method which can drive rapidly large Doppler frequency shift, such as the range of 5 times of symbol rate into the range of 0.35 times of symbol rate. We then consider the non-coherent reception of M-ary/SSMA signal. Since the influence of the Doppler frequency shift is still remain, we propose a scheme that is based on the simultaneous transmission of the two distinctive H-codes. These two codes are assigned respectively to in-phase and quadrature components of the transmitted signal [9]. It is shown that the proposed scheme can achieve good bit-error-rate performance even in the presence of Doppler frequency shift.

II. The Influence of Doppler Frequency Shift

A. Conventional M-ary/SSMA System Model

In order to examine the influence of Doppler frequency shift, we consider an M-ary/SSMA communication system model as shown in Fig.1 [8].

At the transmitter, the ith H-code $a_i (i = 0, 1, 2, \cdot\cdot, M-1)$ is chosen from M H-codes according to $m(=\log_2 M)$ information bits pattern, and multiplied by signature sequence pn^l which can distinguish each user. The H-code is then transmitted in the form of binary PSK signal.

At the receiver, the received signal is divided into two streams and demodulated with in-phase(I-ch) and quadrature(Q-ch) components and then sampled. Each signal is, then, fed to the Walsh-Hadamard Transformer(WHT) which can correlate the signature sequence. The envelope of WHT outputs is compared and the output which indicates the maximum value is detected as the transmitted H-code.

B. Characteristics of Hadamard Codes

Here we examine the characteristics of H-codes. The Hadamard matrix is a square, $M \times M$ matrix, is generated by Kronecker-product of second order matrix shown as follows,

$$\mathbf{H_2} = \begin{pmatrix} 1 & 1 \\ 1 & -1 \end{pmatrix} \tag{1}$$

$$\mathbf{H_k} = \mathbf{H_{k-1}} \otimes \mathbf{H_2} = \begin{pmatrix} \mathbf{H_{k-1}} & \mathbf{H_{k-1}} \\ \mathbf{H_{k-1}} & -\mathbf{H_{k-1}} \end{pmatrix} \tag{2}$$

where $\otimes$ denotes Kronecker-product operation. Now let us express the matrix by four sub-matrices: $\mathbf{H_U}$,$\mathbf{H_V}$,$\mathbf{H_W}$ and

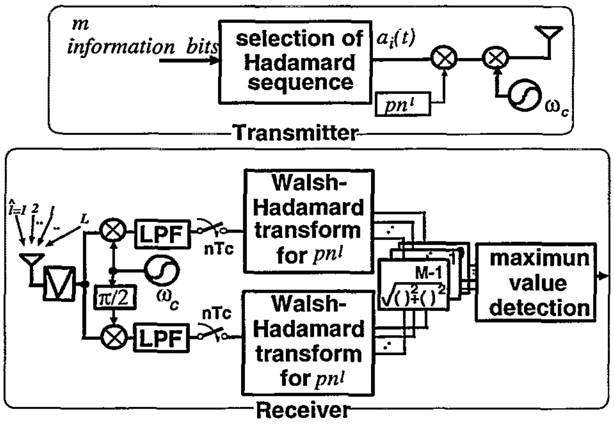

Fig. 1. Conventional M-ary/SSMA system model for user l.

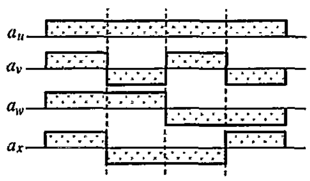

Fig. 2. Pattern of H-codes.

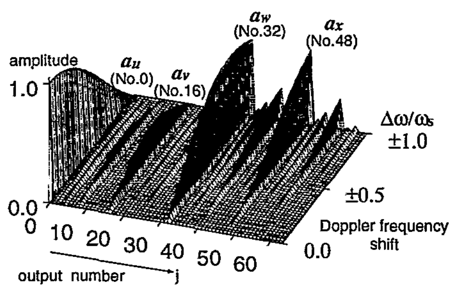

(a) $|\Delta\omega/\omega_s| \leq 1.00$

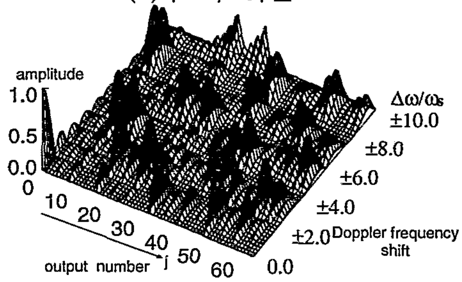

(b) $|\Delta\omega/\omega_s| \leq 10.0$ j

Fig. 3. Example of the influence of Doppler frequency shift.

$\mathbf{H_X}$. These four sub-matrices are,

$$\mathbf{H_k} = \begin{matrix} \mathbf{H_u}: \\ \mathbf{H_V}: \\ \mathbf{H_W}: \\ \mathbf{H_X}: \end{matrix} \begin{pmatrix} \mathbf{H_{k-2}} & \mathbf{H_{k-2}} & \mathbf{H_{k-2}} & \mathbf{H_{k-2}} \\ \mathbf{H_{k-2}} & -\mathbf{H_{k-2}} & \mathbf{H_{k-2}} & -\mathbf{H_{k-2}} \\ \mathbf{H_{k-2}} & \mathbf{H_{k-2}} & -\mathbf{H_{k-2}} & -\mathbf{H_{k-2}} \\ \mathbf{H_{k-2}} & -\mathbf{H_{k-2}} & -\mathbf{H_{k-2}} & \mathbf{H_{k-2}} \end{pmatrix}. \quad (3)$$

Observing the above sub-matrices, it is clear that each sub-matrix consists of the same $\mathbf{H_{k-2}}$ matrix, and the difference is only in the sequency. Here, we define the sequency as a number of sign changes, i.e., positive to negative or vice versa [10]. The difference in the number of sequencies between $\mathbf{H_u}$ and $\mathbf{H_W}$ is one and between $\mathbf{H_V}$ and $\mathbf{H_X}$ is also one. We, further, express a_u as an H-code which belongs to $\mathbf{H_u}$. Similarly, a_v,a_w and a_x are the H-codes which belong to $\mathbf{H_V}$,$\mathbf{H_W}$ and $\mathbf{H_X}$, respectively. Figure 2 illustrates H-codes a_u,a_v,a_w and a_x.

The subscripts indicate the H-codes number and they have the following relations,

$$v = u + \frac{M}{4}, \;\; w = u + 2 \times \frac{M}{4}, \;\; x = u + 3 \times \frac{M}{4}. \quad (4)$$

C. Influence of Doppler Frequency Shift

Figure 3 shows an example of the effect of Doppler frequency shift. Figure 3(a) shows the effect of Doppler frequency shift in the case of $|\Delta\omega/\omega_s| \leq 1.0$ and Fig.3(b) shows in the case of $|\Delta\omega/\omega_s| \leq 10.0$, where $\Delta\omega$ is the Doppler frequency shift and ω_s is the H-code symbol rate. In these figures, we set $M = 64$ and transmitted H-code is a_0, which belongs to $\mathbf{H_u}$. In addition, we assume noiseless channel. As it can be seen from Fig.3(a), the amplitude of the desired uth signal decreases as the Doppler frequency shift increases. On the other hand, the increase in the Doppler frequency shift causes increase in undesired signal amplitude. In particular, the dominant effect can be found in a_w because the difference in the number of sequencies a_u and a_w is one, as shown in Fig.2. As shown in Fig.3(b) , the amplitude of each output number appears even in large Doppler frequency shift, which is contrast with DS/SS scheme. Furthermore the patterns of the amplitudes of WHT are corresponded to the value of Doppler frequency shift.

Figure 4 shows the relation between the transmitted H-code and the amplitudes to evaluate the influence of Doppler frequency shift of WHT for the case of small Doppler frequency shift, i.e. $\Delta\omega/\omega_s = 0$ and 0.5. In the absence of Doppler frequency shift, as shown in Fig.4(a), relation of transmitted sequence and output number is one to one. For $\Delta\omega/\omega_s = 0.5$, the dominant effect of Doppler frequency shift is found on the output numbers of $j = i + \frac{M}{4}, i + \frac{M}{2}, i + \frac{3M}{4}$ when H-code a_i is transmitted, and the output numbers of $j = i$ and $j = i + \frac{M}{2}$ are the same. Therefore, the effect of Doppler frequency shift affects H-codes whose difference in sequencies is small.

With the above mentioned observations, we propose an initial carrier frequency acquisition method and an M-ary/SS scheme which can mitigate the effect of Doppler frequency shift. The proposed initial carrier frequency acquisition method can be used as discussed above in Fig.3(b), and hence an M-ary/SSMA scheme can be proposed from the discussions of Fig.3(a) and Fig.4.

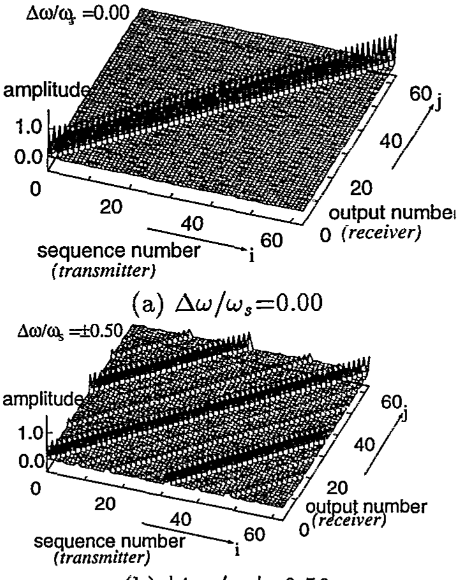

(a) $\Delta\omega/\omega_s$=0.00

(b) $|\Delta\omega/\omega_s|$=0.50

Fig. 4. Relation between transmitted H-code and amplitudes.

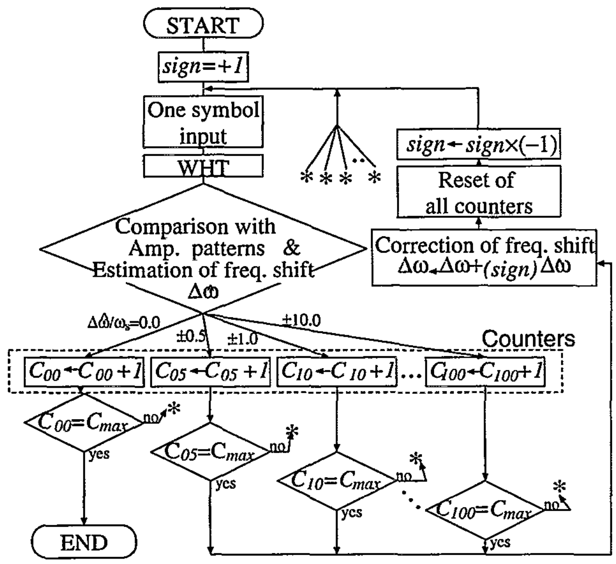

Fig. 5. Flowchart of the initial carrier frequency acquisition scheme.

III. Proposal of New Initial Carrier Frequency Acquisition Method and New M-ary/SSMA Scheme

A. Proposal of Initial Carrier Frequency Acquisition Method

Figure 5 shows the flowchart of new initial carrier frequency acquisition method. In this figure, $\Delta\hat{\omega}/\omega_s$, i.e., the Doppler frequency shift normalized by symbol rate is estimated. $C_{00}, C_{01}, \cdots, C_{100}$ are the values of counters and C_{max} is the threshold of counter. In this method, preamble symbols consisting of H-code a_0 are used for the acquisition and these symbols are demodulated by the receiver as is

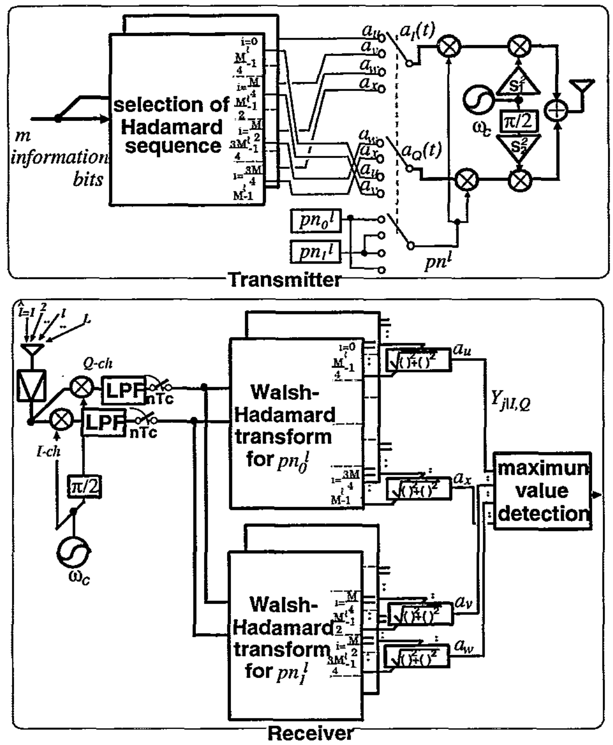

Fig. 6. New M-ary/SSMA system model.

shown in Fig.1. First, one symbol duration of preamble symbol is demodulated by WHT. The output signal is compared with every amplitude pattern. The amplitude patterns are prepared from Fig.3(b) and the frequency resolution normalized by symbol rate is 0.5. The amplitude pattern which is very close to the WHT output levels is selected and the estimated frequency shift $\Delta\hat{\omega}/\omega_s$ is detected according to the selected amplitude pattern. The counter C_{10}, for example, is increased by one when the estimated frequency shift $\Delta\hat{\omega}/\omega_s$ is ±1.0, similarly, the other counters, the value of counter is increased by one corresponding to their estimated frequency shift. After repeating above action, if the value of one of the counters achieves the threshold C_{max}, the Doppler frequency shift is corrected and all counters are reset. Repeating these actions, the estimation of Doppler frequency shift is completed when the value of counter C_{00} achieves the threshold C_{max}.

By the way, the sign of Doppler frequency shift can not be estimated because only amplitude patterns are used for estimation. Therefore, we prepare the variable *sign* in this flowchart and the change of *sign* can estimate the Doppler frequency shift in both positive and negative cases.

B. Proposal of New M-ary/SSMA Scheme

In this subsection, we propose a new M-ary/SSMA scheme that can mitigate the influence of Doppler frequency shift. The new M-ary/SSMA scheme is based on the simultaneous transmission of two H-codes having difference of one in the sequencies[9]. We explain the effect of the simultaneous transmission and then analyze the bit-error-rate performance

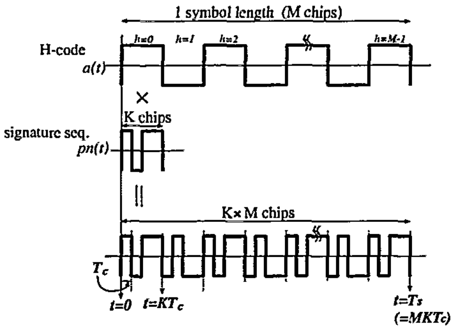

Fig. 7. Relation between H-code and signature sequence.

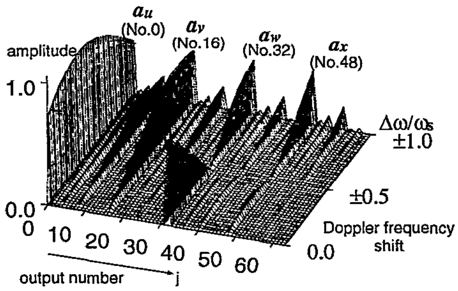

$(S_1^2 : S_2^2$=0.5:0.5)

Fig. 8. Example of the effect of simultaneous transmission.

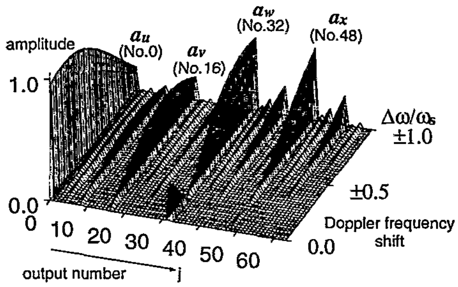

$(S_1^2 : S_2^2$=0.9:0.1)

Fig. 9. Effect of unequal signal power assignment.

of the proposed scheme.

B.1 Proposed M-ary/SSMA System Model

Figure 6 shows the system model of proposed M-ary/SSMA scheme. At the transmitter, the ith and the $(i+\frac{M}{2})$th H-codes are chosen from M H-codes according to m information bits. The chosen two H-codes are assigned respectively to in-phase and quadrature components, which is denoted as $[a_I^l, a_Q^l]$. We, hereafter, denote $[a_I^l, a_Q^l]$ as the H-code set. Since the chosen H-codes have the difference of one in the sequencies, there can be four H-code sets : $[a_u, a_w], [a_v, a_x], [a_w, a_u]$ and $[a_x, a_v]$. The chosen H-code set is, then, multiplied by signature sequence. To distinguish between $[a_u, a_w]$ and $[a_w, a_u]$ or $[a_v, a_x]$ and $[a_x, a_v]$, H-code sets $[a_u, a_w]$ and $[a_x, a_v]$ are multiplied by pn_0^l and $[a_w, a_u]$ and $[a_v, a_x]$ are multiplied by pn_1^l, i.e., one user have two signature sequences. Then, this H-code set is transmitted in the form of quadrature PSK signal.

At the receiver, the received signal is divided into two streams and demodulated with in-phase and quadrature components and then sampled, respectively.

Each demodulated signal is fed to WHT. Since the transmitted H-code set is multiplied by one of the two signature sequences, we need two WHTs, out of which one can correlate to pn_0^l and the other to pn_1^l.

Finally, the envelope which indicates the maximum value is detected as the transmitted H-code set.

The relation between H-code and signature sequence is shown in Fig.7. Here we have set the duration of signature sequence equals to the chip duration of H-code in this system, i.e., if the chip duration of signature sequences is T_c, the chip duration of H-code is KT_c and the symbol duration of H-code is MKT_c, where K is the number of chips of signature sequence. The reason for this setting is that the influence of the Doppler frequency shift becomes much smaller as the duration of signature sequences becomes much smaller than the symbol duration of H-code. Moreover, for such a setting, the Fast Walsh-Hadamard transform can be applied.

B.2 The Effect of Unequal Signal Power Assignment

Figure 8 shows an example of the influence of the Doppler frequency shift at the simultaneous transmission where the transmitted H-code set is $[a_I, a_Q] = [a_0, a_{32}]$, which belongs to $[a_u, a_w]$. The effect of noise is not considered here to simplify the discussion and again M is set to 64. We observe that when $\Delta\omega/\omega_s = 0.0$, the amplitude of the desired uth signal is $1/\sqrt{2}$ and it increases as $\Delta\omega/\omega_s$ increases and when $\Delta\omega/\omega_s = 0.5$, it reaches the maximum, i.e., ≈ 1.0 and then starts to decrease. In contrast to the conventional system, as shown in Fig.3(a), the simultaneous transmission in the proposed scheme shows rather poor performance when the influence of the Doppler frequency shift is small. To improve this poor characteristic, we assign unequal signal power of in-phase and quadrature components.

Figure 9 shows examples of the effect of the Doppler frequency shift with different signal power when H-code set is $[a_0, a_{32}]$. Note that $S_1^2 + S_2^2 = 1$ and we consider the case of $S_1^2 \geq S_2^2$. As it can be shown from this figure, the degradation of the amplitude of desired signal is smaller than that is shown in Fig.8 when the influence of the Doppler frequency shift is small. From this figure, we also observe that the dominant effect of undesired amplitudes is found in a_v, and a_x, which belong to $\mathbf{H_V}$ and $\mathbf{H_X}$, and the largest effect is with a_v. Since we simultaneously transmit a_w, it is not necessary to consider the undesired effect of a_w.

B.3 Bit-Error-Rate Performance Analysis

As it can be seen from Fig.9, the largest effect of carrier frequency offset is found in the amplitude of the xth output because a_w is transmitted with a_u simultaneously and the amplitude of the vth output little appears due to the difference of signature sequence. Therefore, we can assume p.d.f.s of uth and xth outputs to be Rice distribution and the rest to be Rayleigh distribution under the AWGN channel [8][11].

The probability that the H-code set $[a_u, a_w]$ is transmitted but the jth output level is larger than the desired uth output level is given by [11],

$$Pe_{j|u,w} = \int_0^\infty \mathbf{p}(Y_{u|u,w}) \int_{Y_{u|u,w}}^\infty \mathbf{p}(Y_{j|u,w}) dY_{j|u,w} dY_{i|u,w}$$

$$= \begin{cases} \int_0^\infty \frac{Y_{u|u,w}}{N} exp\left[-\frac{Y_{u|u,w}^2 + A_{u|u,w}^2}{2N}\right] \mathrm{I}_0\left(\frac{A_{u|u,w}Y_{u|u,w}}{N}\right) \\ \quad \times Q\left(\frac{A_{x|u,w}}{\sqrt{N}}, \frac{Y_{u|u,w}}{\sqrt{N}}\right) dY_{u|u,w}, & (\text{if } j = x) \\ \frac{1}{2} exp\left[-\frac{A_{u|u,w}^2}{4N}\right] & (\text{if } j \neq x) \end{cases} \quad (5)$$

where $\mathbf{p}(\bullet)$ denotes the p.d.f., $Y_{j|u,w}$ is the envelope of the jth outputs, $\mathrm{I}_0(\alpha)$ is the modified Bessel function of the first kind and zero-th order, and $Q(\alpha, \beta)$ is Marcum's Q function. $A_{u|u,w}$ and $A_{x|u,w}$, the amplitudes of the uth and xth outputs in the case of noise free, are given by,

$$A_{u|u,w}\left(\frac{\Delta\omega}{\omega_s}\right) = \frac{1}{\pi}\frac{\omega_s}{\Delta\omega}\left|S_1 \sin\left(\pi\frac{\Delta\omega}{\omega_s}\right) - S_2\left(\cos\left(\pi\frac{\Delta\omega}{\omega_s}\right) - 1\right)\right| \quad (6)$$

$$A_{x|u,w}\left(\frac{\Delta\omega}{\omega_s}\right) = \frac{1}{\pi}\frac{\omega_s}{\Delta\omega}\left|S_2\left(2\cos\left(\frac{\pi}{2}\frac{\Delta\omega}{\omega_s}\right) - 1 - \cos\left(\pi\frac{\Delta\omega}{\omega_s}\right)\right) + S_1\left(\sin\left(\pi\frac{\Delta\omega}{\omega_s}\right) - 2\sin\left(\frac{\pi}{2}\frac{\Delta\omega}{\omega_s}\right)\right)\right|. \quad (7)$$

When $S_1^2 : S_2^2$=1.0:0.0, the normalized value of $A_{u|u,w}(0) = 1$. N is the normalized received noise power.

Since all H-code sets are transmitted independently with equal probabilities, we obtain the bit-error-rate in the presence of Doppler frequency shift as follows,

$$Pe = \frac{2^{M/2}}{2^M - 1}\left[1 - \left(1 - \frac{1}{2}exp\left[-\frac{A_{u|u,w}^2}{4N}\right]\right)^{M-2} \times \left(1 - Pe_{x|u,w}\right)\right]. \quad (8)$$

IV. Numerical Result

To confirm the above discussions, we evaluate the effectiveness of the proposed initial carrier frequency acquisition method and the new M-ary/SSMA scheme.

A. Performance of the Acquisition Method

Figure 10 shows the estimation error probability of the initial carrier frequency acquisition method in the case of

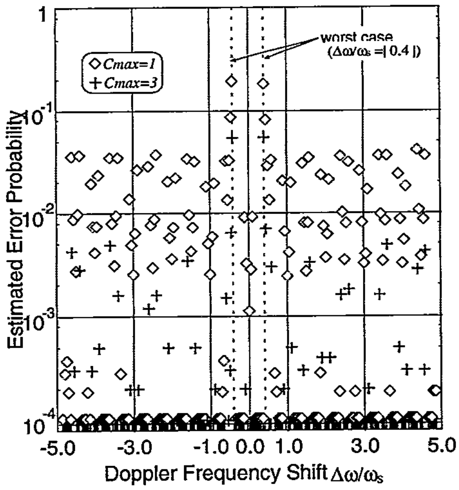

Fig. 10. Estimated error probability with Doppler frequency shift.

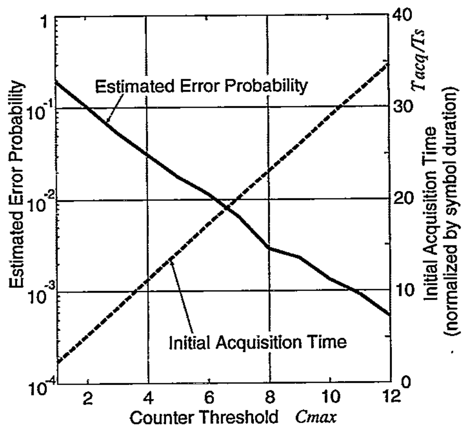

Fig. 11. Relation between estimated error probability and C_{max}.

C_{max}=1 and 3. We set E_b/N_0=6dB, M=64, K=32 and L=1 (no-interference). Furthermore, we plot the estimated error probability values less than at 10^{-4}. We assume the estimation of Doppler frequency shift successes when the Doppler frequency shift can be driven into $|\Delta\omega/\omega_s| \leq 0.35$. It can be observed that the the estimated error probability is the worst in the case of $|\Delta\omega/\omega_s| = 0.40$. It can be also observed that different results of the error probability can attain to less than 10^{-4} even when C_{max} is 1.

Figure 11 shows the estimated error probability and the acquisition time when C_{max} changes. T_{acq}/T_s is the initial acquisition time normalized by symbol duration. In this figure, the Doppler frequency shift $|\Delta\omega/\omega_s|$ is 0.40, which is the worst case. It can be observed that the increase in the threshold C_{max} improves the performance of estimated error probability. This increase, however, degrades the value of the acquisition time. As the result, we must set C_{max}=11 and about T_{acq}/T_s=30 preamble symbols are necessary for the acquisition if we assume the estimated error probability is less than 10^{-3}.

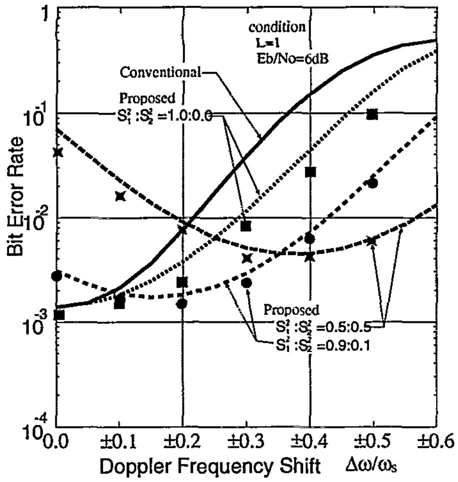

Fig. 12. Bit-error-rate performance of proposed M-ary/SSMA scheme.

B. Bit-Error-Performance of Proposed M-ary/SSMA Scheme

Figure 12 shows the bit-error-rate performance of the proposed and the conventional M-ary/SSMA schemes. Both analysis and simulation results are plotted in this figure, where E_b/N_0=6dB and number of users is L=1. The number of chips for one symbol for the proposed scheme is 2032($=M \times K$).

In the case $\Delta\omega/\omega_s = 0.0$, we found a slight degradation in the proposed scheme due to the energy loss in the quadrature component, S_2^2.

In the presence of Doppler frequency shift, we have observed the performance improvement with the proposed scheme. When the range of value of $\Delta\omega/\omega_s$ is greater than about 0.3, the increase in the quadrature component signal power, S_2^2 improves the bit-error-rate performance. The large effect of the improvement due to S_2^2, however, is not expected.

Therefore, we conclude that the power ratio which is suited for the proposed scheme is $S_1^2 : S_2^2 \approx 0.9 : 0.1$.

V. Conclusions

In this paper, we have discussed a non-coherent reception of M-ary/SSMA signals in the presence of large Doppler frequency offset.

As the result, we found that the new initial acquisition scheme can drive the large value of Doppler frequency shift into the small value, less than 0.35 times of symbol rate. We also found the proposed M-ary/SSMA scheme to be effective in reducing the degradation caused by the Doppler frequency shift. The assignment of unequal signal powers to in-phase and quadrature components could reduce the degradation of the performance due to the Doppler frequency shift. Especially, in the case $S_1^2 : S_2^2 = 0.9 : 0.1$, the performance has been improved in the range of Doppler frequency shift up to 0.35 times of symbol rate.

We concluded that the proposed initial acquisition method and the proposed M-ary/SSMA scheme are suited for the LEO satellite communication systems.

References

[1] K.S. Gilhousen, I.M. Jacobs, R. Padovani, and L.A. Weaver,JR., "Increased Capacity Using CDMA for Mobile Satellite Communication," IEEE Journal on S.A.C., Vol.8, No.4., pp.503–514, May 1990.

[2] M. Katayama, A. Ogawa, and N. Morinaga, "Satellite Communication Systems with Low-Earth-Orbits and the Effects of Doppler Shift," IEICE Trans. Commun., (Japanese), Vol.J76-B-II, No5, pp.382–309, May 1993.

[3] S. Tachikawa and G. Marubayashi, "Spectral Efficiency of M-ary/Spread Spectrum Multiple Access Communication Systems," IEICE Trans. Fund., (Japanese), Vol.J73-A, No.10, pp.1678–1687, October 1990.

[4] R.D. Gaudenzi, T. Garde, F. Giannetti, and M. Luise, "A Performance Comparison of Orthogonal Code Division Multiple-Access Techniques for Mobile Satellite Communications," IEEE Journal on S.A.C., Vol.13, pp.325–332, February 1995.

[5] G. Hakizimana and G. Jourdain, "A New M-ary Wideband Communication System with Application to Multipath Channels - Part I: System Performance," IEEE Trans. on Commun., Vol.COM-43, No.1, pp.127–134, January 1995.

[6] L.M.A. Jalloul and J.M. Holtzman, "Performance Analysis of DS/CDMA with Noncoherent M-ary Orthogonal Modulation in Multipath Fading Channels," IEEE Journal on S.A.C., Vol.12, No.5, pp. 862–870, June 1994.

[7] A.L. Kachelmyer and K.W. Forsythe, "M-ary Orthogonal Signaling in the Presence of Doppler," IEEE Trans. on Commun., Vol.COM-41, No.8, pp.1192–1200, August 1993.

[8] T. Wada, T. Yamazato, M. Katayama, and A.Ogawa, "Non-coherent Reception of M-ary/Spread-Spectrum Signals in the Presence of Carrier Frequency Offset," IEICE Trans. Fund., Vol.E78-A, No.9, pp.1102–1108, September 1995.

[9] T. Wada, T. Yamazato, M. Katayama, and A. Ogawa, "A Study on Non-Coherent Reception of M-ary/Spread-Spectrum Signals in the Presence of Carrier Frequency Offset," Proc. of ICUPC'95, B5.5, pp.412-416, November 1995.

[10] M. Kasahara and H. Tanaka, Digital Communication Systems, Shoko-do(Japanese), 1992.

[11] S. Stein and J.J. Jones, Modern Communication Principle, McGraw hill, 1967.